7 July 2000

ELSEVIER

Chemical Physics Letters 324 (2000) 240–248

CHEMICAL PHYSICS LETTERS

www.elsevier.nl/locate/cplett

The effect of parent zero-point motion on the ND_2 $(\tilde{A})$ rotational state distribution in the 193.3 nm photolysis of ND_3

Jonathan P. Reid, Richard A. Loomis [1], Stephen R. Leone [*,2]

JILA, National Institute of Standards and Technology and University of Colorado, Department of Chemistry and Biochemistry, University of Colorado, Boulder, CO 80309-0440, USA

Received 31 March 2000; in final form 8 May 2000

Abstract

The vibrational and rotational product-state distributions of $ND_2(\tilde{A}\,^2A_1)$ has been probed following the photodissociation of ND_3 at 193.3 nm by time-resolved Fourier Transform infrared emission spectroscopy. The dynamics of the bond cleavage are inferred from the product state distributions by comparison with an earlier study of the photodissociation of NH_3. The degree of excitation about the minor rotational b/c-axes of the product is attributed to the amount of zero-point energy of the parent molecule in the ν_4 H–N–H (D–N–D) scissors bending coordinate of the $NH_3/ND_3(\tilde{A})$ predissociative state. A bimodal $ND_2(\tilde{A}\,^2A_1)$ distribution is observed for rotation about the primary a-axis, analogous to the NH_2 fragment formed in the photodissociation of NH_3.

1. Introduction

Probing the product state distribution following the photofragmentation of a molecular species is a powerful method for characterizing the mechanism by which bond cleavage occurs. Recently, we examined the dissociation mechanism of ammonia, NH_3, from its first excited electronic state $(\tilde{A}\,^1A''_2)$ by time-resolved Fourier transform infrared (FTIR) spectroscopy [1]. By probing the emission from the electronically excited $NH_2(\tilde{A}\,^2A_1)$ fragments, the partitioning of energy into the rotational and bending vibrational levels of the product was determined. In particular, the dynamics leading to rotation around both the a-axis and b/c-axes were explored in a supersonic jet-cooled expansion of the parent species, which minimizes the influence of parent rotational excitation on the bond cleavage dynamics. This extended the results of an earlier study of dissociation at room temperature, in which the degree of rotational excitation about the primary rotational a-axis was probed [2].

Other studies have probed in detail both experimentally (see, e.g., Refs. [3–6] and references therein) and theoretically [7–9] the energy partitioning in the ground electronic state photoproducts, $NH_2(\tilde{X}\,^2B_1)$. These yield complementary informa-

* Corresponding author. Fax: +1-303-492-5504; e-mail: srl@jila.colorado.edu

[1] National Research Council Research Associate, National Institute of Standards and Technology. Current address: Department of Chemistry, Campus Box 1134, Washington University, One Brookings Drive, Saint Louis, MO 63130-4899, USA.

[2] Staff member, Quantum Physics Division, National Institute of Standards and Technology.

0009-2614/00/$ - see front matter
PII: S0009-2614(00)00605-9

tion to the studies that probe the $\tilde{A}$ state fragments and provide insights into the competition between adiabatic and non-adiabatic electronic state dynamics. The electronically excited $NH_3(\tilde{A}\,^1A''_2)$ parent correlates with the ground state $NH_2(\tilde{X})$ product species at planar geometries while the excited state $NH_2(\tilde{A})$ product correlates with the ground state $NH_3(\tilde{X}\,^1A_1)$. At non-planar geometries, however, the total symmetry of these states is the same ($^1A'$) and an avoided crossing of the states occurs. Thus, the parent molecule can dissociate diabatically at planar geometries to the ground state product, while at non-planar geometries, adiabatic dissociation leads to the excited electronic state $NH_2(\tilde{A})$ fragment and a non-adiabatic dissociation leads to a ground state fragment $NH_2(\tilde{X})$.

In our earlier study on the photodissociation of NH_3, a bimodal rotational distribution was observed about the *a*-axis of the $NH_2(\tilde{A}\,^2A_1)$ product [1]. We suggested that the origin of the bimodal distribution is competition between two distinct mechanisms of dissociation that sample different regions of the potential energy surface. In addition, we suggested that the competition between tunneling and direct dissociations may play a significant role in determining the product energy partitioning. The Franck–Condon (FC) region accessed in the excitation step with a pyramidal geometry is classically bound along the dissociation coordinate and dissociation can only occur by tunneling through the barrier to bond cleavage. In contrast, as the molecule evolves away from bent pyramidal geometries, the dissociation barrier diminishes and the molecule can dissociate directly at a planar geometry. To further probe the role of tunneling and direct dissociations, we present here a study of the photodissociation dynamics of ND_3. By deuterating the parent molecule we anticipate a change in efficiency for any tunneling dissociation that may occur. In probing the $ND_2(\tilde{A})$ fragment, we observe a qualitatively similar bimodal rotational distribution, but with quantitative differences in the relative populations of high and low rotational states.

Jet-cooling the parent molecules to ~ 10 K shows that the rotational energy about the minor *b*/*c*-axes does not arise simply as a consequence of carry-over of parent rotational excitation to products, but may have a dynamic origin. For jet-cooled NH_3, the $NH_2(\tilde{A})$ product was found to have a rotational temperature of 120 ± 15 K about the minor axes [1]. This can be rationalized by considering the effect of vibrational zero-point motion in the parent molecule on the dissociation dynamics. Specifically, the rotational excitation is attributed to a mapping of the zero-point bending motion in the ν_4 H–N–H scissors bending coordinate of the $NH_3(\tilde{A})$ predissociative state onto the $NH_2(\tilde{A}) + H$ photofragments [7]. The motion in this bending coordinate allows the trigonal symmetry of the parent molecule to be broken and permits a torque to be exerted about the *b*/*c* rotational axes of the product as the dissociating bond stretches. This hypothesis, which is based on theoretical calculations [7], is tested further here by probing the rotational excitation of $ND_2(\tilde{A})$ about the minor axes when ND_3 is photodissociated in a jet-cooled expansion. By deuterating the parent molecule, the zero-point energy is reduced and hence the zero-point bending amplitude. The $ND_2(\tilde{A})$ *b*/*c*-axes rotational temperature is found to be 81 ± 11 K. The lower degree of rotational excitation for $ND_2(\tilde{A})$ compared to $NH_2(\tilde{A})$ is believed to be a result of the smaller amplitude of the zero-point motion of $ND_3(\tilde{A})$ compared to $NH_3(\tilde{A})$.

Although experiments have also been performed to probe the ground electronic state fragments in the photodissociation of ND_3, ND_2H and NH_2D [6,10–12], there have been no studies of deuterated ammonia to determine the energy partitioning of the fragments in the excited electronic state. We recently undertook such a comprehensive study, and the fully and partially deuterated parent molecules provide a wealth of information on the photofragmentation dynamics of ammonia, especially when compared with the dissociation of non-deuterated NH_3. In this paper we focus on the results of the photodissociation of ND_3 at a wavelength of 193.3 nm.

2. Experimental

A detailed description of the experimental apparatus has been given in a previous publication and only a brief summary will be presented here [1]. Studies are performed both at room temperature, with a continuous flow of ammonia, and jet-cooled, with a piezoelectric pulsed valve. The triggering of the ArF

excimer laser, which initiates the photodissociation, and the opening of the pulsed valve for the jet-cooled studies, are both synchronized to the position of the moving mirror of a commercial continuous-scan Fourier Transform infrared (FTIR) spectrometer. Following the laser pulse, emission from the electronically excited ND_2 fragments is collected and imaged from the gas flow into the FTIR spectrometer with a CaF_2 lens/mirror telescope arrangement. The emission is modulated by the interferometer and recorded by a detector. Boxcar integrators are used to record several time windows of the fluorescence at each interferogram position and the time history of the entire interferogram is constructed by pulsing the piezoelectric pulsed valve and the laser once for each interferogram position. A total of 16 coadditions are recorded for each spectrum. The time-dependent modulated signal is stored on a computer following analog-to-digital conversion.

The $ND_2(\tilde{A}\,^2A_1 \rightarrow \tilde{X}^2B_1)$ electronic emission is observed over the spectral range 6000–15 000 cm^{-1}. To acquire a complete spectrum over this broad frequency range, the experiment is repeated under identical experimental conditions with two detectors, an InSb detector, for the range 6000–12 000 cm^{-1}, and a Si avalanche photodiode for the range 10 000–15 000 cm^{-1}. A matched detector is used to monitor the total unmodulated emission intensity, and the modulated signal is then corrected for variations in the laser power and gas flow using this second normalization channel. A complete spectrum with a Nyquist frequency of 15 798 cm^{-1} is acquired with a spectral resolution of 0.2 cm^{-1}.

Extensive experiments were performed earlier to characterize the jet-cooled expansion for NH_3 [1]. Only the conclusions crucial to the study presented here are mentioned. It is important to ensure that the dilution of ammonia in a helium buffer gas is sufficient to avoid clustering of the parent molecules. In addition, the backing pressure of the pulsed valve must be sufficiently low to avoid clustering. With an orifice diameter of 750 μm, no evidence of clustering was observed with concentrations of $\leqslant 2\%$ NH_3 in He and with backing pressures of less than 100 kPa. Similar experiments with an expansion of NH_3 in Ar and an orifice of 1 mm showed that the rotational temperature of the jet-cooled parent molecule was < 10 K [13,14]. Therefore, with the improved conditions used in our study, we have concluded that the rotational temperature of the parent molecules is also < 10 K. In the experiments presented below, a concentration of 2% ND_3 in helium was used with a backing pressure of ~ 67 kPa.

In both studies, with a room-temperature continuous reagent flow and with a jet-cooled expansion, no time dependence is observed in the product rotational level distribution from 20 ns out to 2 μs after the photolysis pulse. The $ND_2(\tilde{A})$ excited state rovibrational populations obtained under these conditions represent the nascent values prior to any collisional relaxation.

3. Spectroscopy and product state analysis

Numerous experimental and theoretical investigations of the $NH_2\tilde{A} \rightarrow \tilde{X}$ emission spectrum have been published (see, e.g., Refs. [15–17]). However, the emission spectrum of $ND_2\tilde{A} \rightarrow \tilde{X}$ is much less well characterized. Indeed, the relevant term energies and transition probabilities are unknown for the transitions observed in this study that originate from the electronically excited nascent product levels populated. By comparison with the spectroscopy of NH_2, the observed spectral lines are attributed to rotational transitions within the vibrational bands originating from $v_2' = 0$, 2_0^0, 2_1^0, 2_2^0, 2_3^0 and 2_4^0, where the superscript denotes the vibrational level of the excited electronic state and the subscript that of the ground state. The rovibrational selection rules for all of the electronic transitions used in this spectral analysis follow those of a symmetric prolate top [18]; the change in the total rotational angular momentum, $\Delta N = \pm 1$, equals the change in rotational quanta about the a-axis, i.e. $\Delta N = \Delta K_a = \pm 1$. Rotational angular momenta about the axes of rotation other than the a-axis, referred to collectively as rotation about the b/c-axes, is given by those values of N' for which $N' > K_a'$. Therefore, using the notation for absorption, the emission spectrum is dominated by vibrational bands with ${}^P\mathrm{P}(N'', K_a'')$ and ${}^R\mathrm{R}(N'', K_a'')$ rotational lines. The 'P' and 'R' superscripts refer to $\Delta K_a = -1$ and $\Delta K_a = +1$, respectively, and the 'P' and 'R' branches refer to $\Delta N = -1$ and

$\Delta N = +1$. Each rotational transition is further split by spin-rotation coupling into two components, $F_1 \rightarrow F_1$ and $F_2 \rightarrow F_2$.

A full spectral analysis of the vibrational bands 2_0^0, 2_1^0, 2_2^0, 2_3^0 and 2_4^0 will be given in a future publication; only the information needed to elucidate the dynamics occurring during the bond cleavage are discussed here. The method of combination differences was used in order to ensure a correct assignment, by comparison with the known ground electronic state term energies as determined by Mordaunt et al. [6] Based on these ground state term energies, the excited state term energies are determined and presented in Table 1. The assignment was facilitated by comparing the product emission spectra from both the room-temperature and jet-cooled dissociations. In the latter of these two spectra, the dramatic cooling of the parent molecule greatly reduces the congestion of the emission spectra by constraining the parent rotation, and hence the product, to a smaller subset of rotational states. An example of a section of the emission spectra, both in a jet-cooled experiment and in a room-temperature dissociation is shown in Fig. 1.

The relative populations, $n(N', K_a')$, found within each $ND_2(\tilde{A})$ rovibrational level can be in principle determined from the intensities of the ${}^{P}P(N'', K_a'')$ emission lines, I, transition frequencies, ν, Hönl–London factors, $A_{K_a'',N''}$, and theoretically predicted rovibronic transition moments, R, according to [18]

$$n(N', K_a') = \frac{I}{A_{K_a'',N''}|R|^2\nu^3}. \quad (1)$$

The Hönl–London factors, $A_{K_a'',N''}$, appropriate for a perpendicular transition are used [18].

$$A_{K_a'',N''} = \frac{(N''-1+K_a'')(N''+K_a'')}{K_a''(2K_a''+1)} \quad (2)$$

The vibronic intensity factors, R, are not currently known for ND_2 and so correction of the populations for these factors cannot be made. By analogy with the analysis performed on the fragment NH_2 from the photodissociation of NH_3, correction by the vibronic intensity factors is not expected to change the qualitative trends and conclusions of this work, although the quantitative populations will be susceptible to error. To illustrate the change that inclusion of the vibronic intensity factors could make, consider the most intense vibrational bands in the NH_2 emission spectrum, 2_1^0 and 2_2^0, and the transitions from the lowest and highest rotational states in both the P and R bands. The vibronic intensity factors increase by a factor of ~ 2.3 for both the P and R branches of the 2_1^0 vibrational band and by

Table 1
Term energies for the states $ND_2(\tilde{A}, N' = K_a', \upsilon_2' = 0)$ relative to the zero-point energy of the ground electronic state. The values quoted are taken from the 2_0^0 ${}^{P}P$ bands, although values from the 2_0^0 ${}^{R}R$, 2_1^0 ${}^{P}P$ and 2_1^0 ${}^{R}R$ agree within 7 cm^{-1}. The value for the $ND_2(\tilde{A}, N' = K_a' = 0, \upsilon_2' = 0)$ level is taken from the 2_1^0 ${}^{P}P$ band. These term energies are based on the experimental term energies estimated by Mordaunt et al. for $ND_2(\tilde{X}, N'' = K_a'', \upsilon'' = 0)$, which are quoted for completeness [6]. The $N' > K_a'$ term energies are only quoted for those states used in the analysis of the $N' > K_a'$ populations

K_a	Term energy/cm^{-1}					
	$ND_2(\tilde{X}, N'', K_a'', \upsilon'' = 0)$			$ND_2(N', K_a', \upsilon_2' = 0)$		
	$N'' = K_a''$	$N'' = K_a'' + 1$	$N'' = K_a'' + 2$	$N' = K_a'$	$N' = K_a' + 1$	$N' = K_a' + 2$
0	0	11	32	10478	–	–
1	19	40	72	10842	–	–
2	64	96	139	11195	–	–
5	358	421	496	12397	–	–
6	506	581	666	12835	12896	12967
7	679	765	861	13306	13379	13458
8	876	973	1080	13804	13884	–
9	1096	1204	1322	14324	–	–

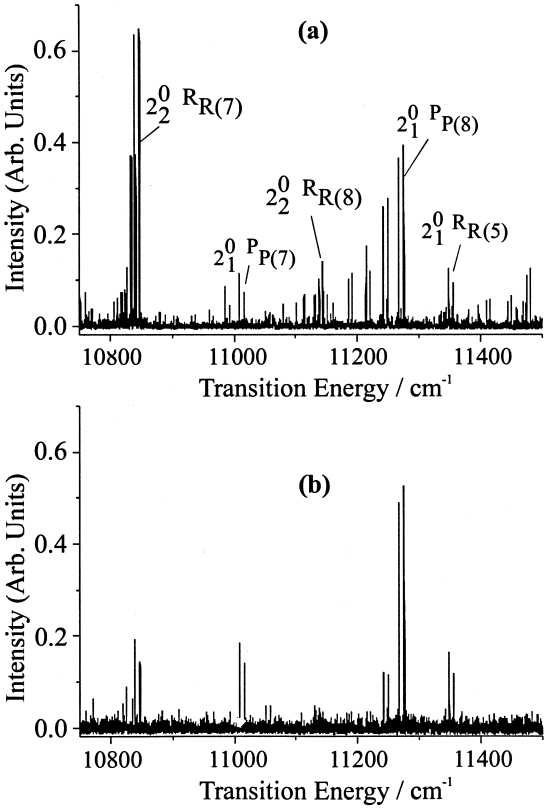

Fig. 1. A section of the photodissociation product emission spectrum of ND_2 ($^2A_1$) from the photodissociation ND_3. (a) Room-temperature dissociation; (b) jet-cooled. Note the significant simplification of the spectra on jet-cooling the parent molecule.

~ 1.8 for the 2_2^0 band on comparing the lowest rotational state with the highest [1,19]. This leads to transitions that are approximately a factor of 4 weaker from the lowest $N' = K'_a$ states relative to the highest. If a similar trend were to be observed in the vibronic intensity factors for ND_2, the population in the lowest $N' = K'_a$ state would increase by a factor of 4, relative to the highest $N' = K'_a$ states, from that calculated in our analysis.

The populations, uncorrected for the vibronic intensity factors, of the product states $ND_2(\tilde{A},\ N' = K'_a,\ v'_2 = 0)$ are shown in Fig. 2. A bimodal rotational distribution is observed with the population peaking in $N' = K'_a = 0$ and 7. Note that the intervening transitions from $N' = K'_a = 3$ and 4 are too weak to be observed within the signal-to-noise of this experiment. The F_1/F_2 spin-rotation components of the transitions are observed with the resolution of the spectrometer, as is seen in Fig. 1, and the average of the F_1 and F_2 rotational level populations are reported. Several vibrational bands originating from the same excited ν_2 vibrational state are observed and the average of the $N' = K'_a$ populations is determined from all of the observed $2^0_{v''}$ bands. The total integrated $ND_2(\tilde{A},\ N' = K'_a,\ v'_2 = 0)$ level population is normalized to one.

To analyze those states with $N' > K'_a$, only the $K'_a = 6$, 7, and 8, $v'_2 = 0$ populations are used. Insufficient signal-to-noise precludes the use of transitions originating from other K'_a states for the determination of the energy partitioning about the minor rotational axes. As in our previous publications, we assume that the vibronic intensity factors are the same for each transition in the series $N' \geqslant K'_a$ for any particular K'_a value. The populations of the $ND_2(\tilde{A},\ N' \geqslant K'_a,\ v'_2 = 0)$ levels are scaled so that the populations in the $N' = K'_a = 6$, 7, and 8 rotor levels divided by the $(2N' + 1)$ state degeneracy each equal one. In our previous examination of the product state distribution following the dissociation

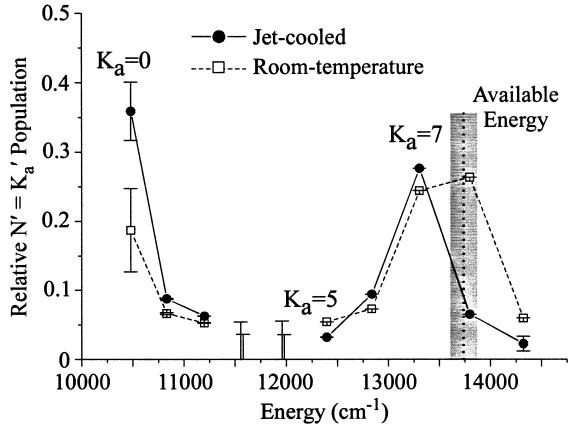

Fig. 2. The relative ND_2 ($v'_2 = 0,\ N' = K'_a$) population distribution obtained by the 193.3 nm photolysis of a room-temperature effusive flow (squares) and jet-cooled expansion (circles) of ND_3. Representative error bars are given to show the upper-limit of the population of the $N' = K'_a = 3$ and 4 states that cannot be observed within the signal-to-noise of this experiment. For these levels, the larger error bars refer to the room-temperature study and the smaller error bars to the jet-cooled, and they are positioned in energy to illustrate only the approximate term energies of these states.

of NH_3, the energy partitioning about the minor axes was best described by a rotational temperature [1,2]. A similar Boltzmann analysis has been performed here to characterize the rotational energy about the b/c-axes and the results of this analysis are illustrated in Fig. 3. To calculate the relative rotational energy about the b/c-axes, the term energies measured by Mordaunt et al. [6] are used for the appropriate states in the ground electronic state. The rotational temperature of the ND_2 product about the b/c-axes is 265 ± 15 K in the room temperature photodissociation of ND_3 and 81 ± 11 K in the jet-cooled studies.

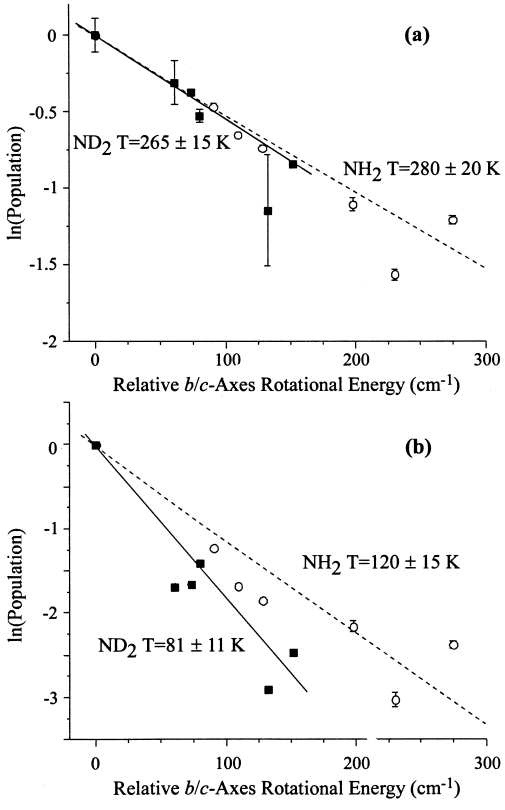

Fig. 3. Boltzmann-type plots of ND_2 ($v_2' = 0$, $N' \geqslant K_a'$) populations (filled squares) following (a) the room-temperature photodissociation of ND_3, and (b) the jet-cooled photodissociation. In both cases, the best fit Boltzmann temperatures are illustrated by the solid line. For comparison, the similar Boltzmann plots for the photodissociation of NH_3 are included (open circles) and the best fit Boltzmann temperature is given by the dashed line.

4. Discussion

In comparison with the dissociation of NH_3, the most striking difference in the photodissociation of ND_3, as illustrated in Fig. 3, is the rotational temperatures about the minor rotational b/c-axes of the $ND_2(\tilde{A})$ fragment in the room-temperature and jet-cooled dissociations. The analysis shows that the rotational temperature of $ND_2(\tilde{A})$, when produced in a room temperature flow of the parent species, is similar to that of $NH_2(\tilde{A})$ from the photodissociation of NH_3 (280 ± 20 K), within their error bars [1]. Since the parent molecule initially has a room temperature rotational distribution, the similarity of these product rotational temperatures suggests that the level of excitation about these minor rotational axes is a result of carry-over of the parent rotational excitation into the product. However, when the parent molecule is cooled to a temperature of < 10 K, the product ND_2 or NH_2 fragment has an elevated level of rotational excitation that cannot simply be a result of carry-over from the parent molecule, but must have an origin in the dynamics occurring during the bond cleavage. The jet-cooled dissociation of both NH_3 and ND_3 show this qualitatively similar trend in the product energy partitioning.

Theoretical calculations by Dixon [7] have shown that zero-point motion in the ν_4 H–N–H scissors bending coordinate of the $NH_3(\tilde{A})$ predissociative state has an amplitude of $\pm 11°$. By considering the mapping of a ground-state Gaussian wavefunction in this coordinate onto the product states, Dixon predicted the population in $NH_2(\tilde{X}, v'' = 0, N'', K_a'')$ states with $N'' > K_a''$. For NH_3, we confirmed that the rotational energy partitioning about the b/c-axes was indeed very similar for $NH_2(\tilde{A}, N' > K_a', v_2' = 0)$ to that predicted from the range of zero-point motion geometries sampled during the dissociation [1], as calculated by Dixon for fragmentation to the ground electronic state product [7]. A schematic, which illustrates this dissociation mechanism, is shown in Fig. 4. Dissociation from the equilibrium geometry in the ν_4 H–N–H scissors bending coordinate of the parent leads to a molecule that retains C_{2v} symmetry during the elongation of the bond being cleaved. By contrast, zero-point motion in this vibrational mode permits the molecule to evolve away from this equi-

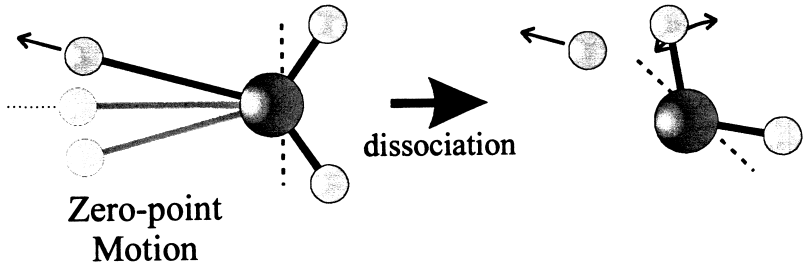

Fig. 4. Schematic showing the origin of the rotational excitation about the minor b/c-axes. A change in the equilibrium geometry that corresponds to the approximate zero-point motion in the $ND_3(\tilde{A})$ ν_4 coordinate breaks the symmetry of the parent molecule and would classically generate a force about the $ND_2(\tilde{A})$ b/c-axes.

librium geometry, thus breaking the C_{2v} symmetry, with the N–H bond elongating in a geometry for which the H-atom moves out of the σ_v symmetry plane. Simple classical arguments show that this would result in a torque and excitation about the minor-rotational axes.

With the qualitative explanation for the excitation about the minor rotational axes being the same, we now consider the quantitative values for the NH_2 and ND_2 product b/c-axes rotational temperatures. The $ND_3(\tilde{A})$ parent molecule has less zero-point energy in the ν_4 D–N–D scissors bending mode than the $NH_3(\tilde{A})$ molecule and therefore less amplitude in the angular bending coordinate. Although the extent of the energy difference cannot be determined for the excited electronic states of the two molecules, from the ground state harmonic frequencies, the zero-point levels differ in energy by 238 cm^{-1}, with energies of 867 and 629 cm^{-1} for NH_3 and ND_3, respectively [11]. Thus, there is a qualitative explanation for the different b/c-axes rotational temperatures of the ND_2 and NH_2. In the former case, the parent ND_3 molecule has less zero-point energy and a smaller bending amplitude and, thus, less torque is induced about the minor rotational axes as the N–D bond cleaves. This is reflected in the lower b/c-axes rotational energy of the $ND_2(\tilde{A})$ product compared to the $NH_2(\tilde{A})$ fragment.

The qualitative trend in the rotational energy partitioning about the major a-axis of $ND_2(\tilde{A})$ is similar to that of $NH_2(\tilde{A})$ from the photodissociation of NH_3. The distributions are bimodal with peaks at both high K_a ($K_a = 5$ for NH_2 and $K_a = 7$ for ND_2), near the energetic limit and at the lowest K_a. It must be reiterated that the population distributions shown in Fig. 2 are not corrected for the vibronic intensity factors, R, of Eq. (2) for the ND_2 rotational transitions. However, by analogy with similar transitions in the spectroscopy of NH_2, the inclusion of this factor will most likely enhance the populations in the lowest K_a states relative to the populations in the high K_a states. Although the populations in the lowest K_a levels are sufficient for transitions originating from these states to be observed, the bimodality of the rotational distribution precludes the observation of the intermediate states with $K_a = 3$ and 4 due to the very small Hönl–London line strength factors for these transitions. A further similarity between the bimodal rotational distributions of $NH_2(\tilde{A})$ and $ND_2(\tilde{A})$ is that, following jet-cooling of the parent molecules, the breadth of the rotational distribution narrows considerably. At room temperature a fraction of the total population is observed in $ND_2(\tilde{A}$, $N' = K'_a = 8$ and 9, $v'_2 = 0)$ where both states lie above the energetically accessible limit for a cold parent molecule. This fraction drops significantly when the thermal rotational energy of the parent molecule is reduced by jet-cooling.

In our previous paper on the photodissociation of NH_3, we suggested that the bimodality of the rotational distribution originates from the competition between two distinct mechanisms for dissociation that sample different geometries during the bond cleavage [1]. Mordaunt et al. performed polarization studies on the photodissociation dynamics of ND_3 to the ground electronic state ND_2 fragment and showed that planar dissociations led to low rotational excitation and non-planar dissociations to high rotational excitation [20]. We concluded in our earlier paper that non-planar geometries accessed in the Franck–

Condon region at an excitation wavelength of 193.3 nm can produce an NH_2 fragment with a high degree of rotational excitation about the *a*-axis [1]. Dissociation from the Franck–Condon region requires bond cleavage by tunneling through the barrier to dissociation. In contrast, dissociation from planar geometries will yield a product fragment with very little *a*-axis rotation and can proceed by direct dissociation over the barrier. Although a direct comparison of the ND_2 and NH_2 rotational distributions is precluded in this study because the ND_2 populations remain uncorrected for the vibronic intensity factor, the inclusion of these factors will likely lead to an enhancement of the population in the low rotational states relative to the high states. This suggests that the ND_2 fragments are born with a lower degree of rotational excitation about the *a*-axis than NH_2, with $ND_2(\tilde{A},\ N' = K'_a = 0,\ 1$ and $2,\ v'_2 = 0)$ dominating in the ND_3 dissociation, but with $NH_2(\tilde{A},\ N' = K'_a = 4,\ 5$ and $6,\ v'_2 = 0)$ dominating the NH_3 dissociation. This could reflect the lower tunneling efficiency of D-atoms when compared with H-atoms during the bond cleavage, and less dissociation from the FC region at non-planar geometries that leads to rotational excitation. In addition, the lower zero-point energy of ND_3 than NH_3 in the ground electronic state suggests that the excitation step leads to an ND_3 molecule that lies lower in energy on the excited state potential energy surface than NH_3. The barrier is, thus, larger to bond cleavage at the large out-of-plane bend angles sampled in the FC region and the molecule is channeled more effectively to planar geometries where the barrier can be surmounted directly without tunneling in the cleavage of the N–D bond. This reduces the extent of rotational excitation about the *a*-axis in the fragment. Previous studies have suggested a disparity in dissociation rates for NH_3 and ND_3 and it was concluded that this difference was due to the differing tunneling efficiencies of H and D atoms [3].

The extent of vibrational energy partitioned into bending excitation of the fragment, $NH_2(\tilde{A},\ v'_2 = 0)/NH_2(\tilde{A},\ v'_2 = 1)$, in the photodissociation of NH_3 was found to be 3:1 under the room-temperature conditions [1]. Since the vibronic intensity factors are similar for transitions from both $v'_2 = 0$ and 1, this population ratio derives directly from the relative ratio of the experimentally observed integrated band intensities of transitions from both $v'_2 = 0$ and 1. In the current study of the photofragmentation of ND_3 only very weak signatures of vibrationally excited ND_2 were observed and these have an insufficient signal-to-noise ratio for a spectroscopic analysis. The relative ratio of the experimental integrated band intensities over all rotational transitions was estimated to be 20:1 for the partitioning $ND_2(\tilde{A},\ v'_2 = 0)/ND_2(\tilde{A},\ v'_2 = 1)$. Although the available energy [11] to the ND_2 fragment is 895 cm^{-1} less than that available to NH_2 for photodissociation at 193.3 nm of ND_3 and NH_3, respectively, this apparent dramatic reduction in the degree of vibrational excitation upon deuteration of the parent molecule cannot be due to an energetic factor. The ND_2 fragment has 3325 cm^{-1} available for partitioning into the internal energy of the excited electronic state fragment. One possible explanation might simply be that the integrated band intensities cannot be compared in this way, since the vibronic intensity factors have not been accounted for. This seems an improbable explanation, as this would require that the oscillator strength for the entire set of rotational transitions from the excited vibrational level must be diminished by close resonances to dark states in the ground electronic state [1]. While such degradation of oscillator strength is observed for certain states in the spectroscopy of $NH_2(\tilde{A})$, only a very small subset of transitions is affected. Thus, the large preference for a $ND_2(\tilde{A},\ v'_2 = 0)$ over a $ND_2(\tilde{A},\ v'_2 = 1)$ product fragment must have a dynamic origin.

Without theoretical calculations to test hypotheses, only significant factors that could influence the dynamics may be tentatively suggested and it is hoped that these will stimulate further theoretical work on these systems. The primary differences in the photodissociation of NH_3 and ND_3 occur in the excitation step. NH_3 undergoes excitation to NH_3 $(\tilde{A}\ ^1A''_2,\ v_2 = 6)$ followed by rapid predissociation that has been suggested to involve a Fermi-resonance between the bending vibration and the symmetric stretch [3]. The ND_3 undergoes excitation to ND_3 $(\tilde{A}\ ^1A''_2,\ v_2 = 7)$ followed by slower predissociation [3]. We suggest that understanding the character of the vibrational mode excited in the parent molecule is essential before any substantive conclusions can be drawn as to the reason for the differences in the vibrational energy partitioning in the products from

the photodissociation of NH_3 and ND_3. In addition, the character of the vibrational mode may significantly influence the regions of the potential energy surface sampled during the dissociation and the possible competition between adiabatic and non-adiabatic dynamics.

Acknowledgements

The authors would like to thank the Department of Energy for support of this research and the National Science Foundation for additional equipment. R.A.L. gratefully acknowledges the support of the National Research Council for a Postdoctoral Fellowship with the National Institute of Standards and Technology. The authors would also like to thank G. Duxbury for invaluable discussions concerning the electronic spectroscopy of NH_2 and ND_2.

References

[1] R.A. Loomis, J.P. Reid, S.R. Leone, J. Chem. Phys. 112 (2000) 658.
[2] E.L. Woodbridge, M.N.R. Ashfold, S.R. Leone, J. Chem. Phys. 94 (1991) 4195.
[3] V. Vaida, M.I. McCarthy, P.C. Engelking, P. Rosmus, H.-J. Werner, P. Botschwina, J. Chem. Phys. 86 (1987) 6669.
[4] J. Biesner, L. Schnieder, J. Schmeer, G. Ahlers, X. Xie, K.H. Welge, M.N.R. Ashfold, R.N. Dixon, J. Chem. Phys. 88 (1988) 3607.
[5] J. Biesner, L. Schnieder, G. Ahlers, X. Xie, K.H. Welge, M.N.R. Ashfold, R.N. Dixon, J. Chem. Phys. 91 (1989) 2901.
[6] D.H. Mordaunt, M.N.R. Ashfold, R.N. Dixon, J. Chem. Phys. 104 (1996) 6460.
[7] R.N. Dixon, Mol. Phys. 88 (1996) 949.
[8] M.I. McCarthy, P. Rosmus, H.-J. Werner, P. Botschwina, V. Vaida, J. Chem. Phys. 86 (1987) 6693.
[9] P. Rosmus, P. Botschwina, H.-J. Werner, V. Vaida, P.C. Engelking, M.I. McCarthy, J. Chem. Phys. 86 (1987) 6677.
[10] S.A. Henck, M.A. Mason, W.-B. Yan, K.K. Lehmann, S.L. Coy, J. Chem. Phys. 102 (1995) 4783.
[11] D.H. Mordaunt, R.N. Dixon, M.N.R. Ashfold, J. Chem. Phys. 104 (1996) 6472.
[12] A. Nakajima, K. Fuke, K. Tsukamoto, Y. Yoshida, K. Kaya, J. Phys. Chem. 95 (1991) 571.
[13] T. Seelemann, P. Andresen, J. Schleipen, B. Beyer, J.J. Ter Meulen, Chem. Phys. 126 (1988) 27.
[14] G. Ebel, R. Krohne, H. Meyer, U. Buck, R. Schinke, T. Seelemann, P. Andresen, J. Schleipen, J.J. ter Meulen, G.H.F. Diercksen, J. Chem. Phys. 93 (1990) 6419.
[15] S.C. Ross, F.W. Birss, M. Vervloet, D.A. Ramsay, J. Mol. Spec. 129 (1988) 436.
[16] C. Jungen, K.-E.J. Hallin, A.J. Merer, Mol. Phys. 40 (1980) 25.
[17] G. Duxbury, R.N. Dixon, Mol. Phys. 43 (1981) 255.
[18] G. Herzberg, Molecular Spectra and Molecular Structure III. Electronic Spectra and Electronic Structure of Polyatomic Molecules, Van Nostrand-Reinhold, New York, 1966.
[19] G. Duxbury, private communication.
[20] D.H. Mordaunt, M.N.R. Ashfold, R.N. Dixon, J. Chem. Phys. 109 (1998) 7659.